

# **The Physics of Plasma Ion Chemistry: A Case Study of Plasma Polymerization of Ethyl Acetate**

*Solmaz Saboohi<sup>1</sup>, Robert D. Short<sup>2</sup>, Bryan Coad<sup>3</sup>, Hans J. Griesser<sup>1</sup>, Andrew Michelmore<sup>1,4\*</sup>*

- 1. Future Industries Institute, University of South Australia, Mawson Lakes Campus, Mawson Lakes, Australia, 5095*
- 2. Materials Science Institute and Department of Chemistry, University of Lancaster, City of Lancaster, UK*
- 3. School of Agriculture, Food and Wine, University of Adelaide, Adelaide, SA 5005, Australia*
- 4. School of Engineering, University of South Australia, Mawson Lakes Campus, Mawson Lakes, Australia, 5095*

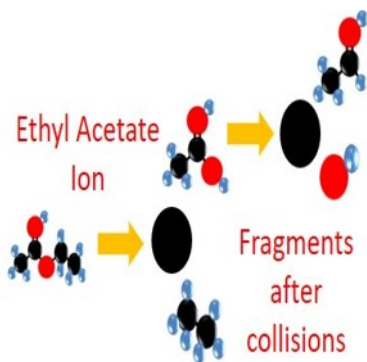
## **Corresponding Author**

\*Andrew Michelmore email: [andrew.michelmore@unisa.edu.au](mailto:andrew.michelmore@unisa.edu.au)

## ABSTRACT

Deposition chemistry from plasma is highly dependent on both the chemistry of the ions arriving at surfaces, and the ion energy. Typically, when measuring the energy distribution of ions arriving at surfaces from plasma, it is assumed that the distributions are the same for all ionic species. Using ethyl acetate as a representative organic precursor molecule, we have measured the ion chemistry and ion energy as a function of pressure and power. We show that at low pressure ( $< 2\text{Pa}$ ) this assumption is valid, however at elevated pressures ion-molecule collisions close to the deposition surface affect both the energy and chemistry of these ions. Smaller ions are formed close to the surface and have lower energy than larger ionic species which are formed in the bulk of the plasma. The changes in plasma chemistry therefore are closely linked to the physics of the plasma - surface interface.

## TOC GRAPHIC



**KEYWORDS** Ion deposition, Plasma polymerization, Ion Energy, Mass Spectrometry, Thin Films

There is much interest in improving understanding of how the physics and chemistry of plasmas vary with external process parameters and in turn affect the outcomes of plasma processing methodologies. In plasma polymerization for example, the composition and properties of polymeric film coatings from a given process vapour can vary considerably,<sup>1</sup> and the relative roles of radicals and ions in the film build-up is one aspect that is in need of more detailed understanding, including which of many possible ions contribute and how their contributions vary with pressure and power. Ions are used to fabricate thin film coatings in ion beam deposition,<sup>2</sup> plasma enhanced atomic layer deposition<sup>3</sup> and grafting,<sup>4</sup> and plasma polymerisation.<sup>5,6</sup> Plasma polymerisation is particularly useful for deposition of films which retain the chemical functionality of the precursor,<sup>7</sup> and has therefore been used in a number of industrial processes. The total film growth rate from plasma can be given by Equation 1,<sup>8</sup>

$$\Gamma_{total} = \sum_{m=0}^{\infty} \Gamma_{m,ions} P_{m,ions} + \sum_{m=0}^{\infty} \Gamma_{m,radicals} P_{m,radicals} + \sum_{m=0}^{\infty} \Gamma_{m,neutrals} P_{m,neutrals}$$

(eq 1)

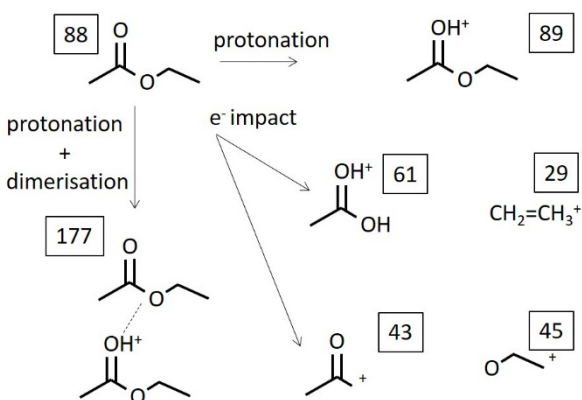
where  $\Gamma_m$  is the flux of each species with mass  $m$ , and  $P_m$  is the net sticking probability of each species including the possibility of etching. The degree to which ions contribute mass to film growth can vary between 1% and nearly 100% depending on the process conditions.<sup>9</sup> In order to maximise retention of chemical functionality, low pressure and power has been historically used to minimise fragmentation in the plasma phase and reduce sputtering and etching of the growing film by reducing the ion energy.<sup>10</sup> In this plasma mode, the sheath region close to surfaces is collision-less, and is known as the alpha regime. This regime has been proven for simple functional groups (e.g. carboxylic acids, amines etc)<sup>11,12</sup> but for more complex functional groups may not be suitable, as the functional group structure can be fragile and unlikely to survive multiple electron impacts while traversing the plasma phase. In this case, ionisation close to the surface can be promoted by increasing the pressure such that ion-molecule collisions occur close to the

surface within the sheath.<sup>13</sup> We have shown recently that by tuning the plasma to this collisional regime (the gamma regime) the mass spectrum of ions arriving at the surface may be biased towards retention of the precursor structure, and functional retention can be enhanced,<sup>14,15</sup> and this has been shown to affect the performance of the film.<sup>16</sup>

The ion energy distribution is also critical in retaining chemical functionality as the kinetic energy with which ions arrive at the surface determines the physico-chemical processes that may occur; low energy ions (< 2eV) may physisorb or elastically scatter, ions with energies between 2-15eV may chemisorb via surface dissociation (so called “soft landing”), while higher energy ions may chemisorb while promoting surface etching, cross-linking and molecular rearrangements.<sup>17</sup> Thus,  $P_m$  in equation 1 is strongly dependent on ion energy, and controlling both the chemistry of the plasma phase and the ion energy distribution is critical.

Here, ethyl acetate plasma is studied to investigate the ion chemistry and energy distribution in the alpha and gamma regimes. Ethyl acetate was chosen as a representative precursor as it has a molecular weight and vapour pressure which are typical of those used in plasma polymerisation, and has a methyl and ethyl group on either side of the ester group enabling easy identification of positive ion fragments and fragmentation pathways. It has been generally assumed that all ionic species arriving at the surface have the same energy distribution. For very low pressures, this is certainly the case as ions created in the bulk of the plasma gain kinetic energy while passing unimpeded through the sheath voltage (typically 20-30V). The mass spectrum of the positive ions from a 10W ethyl acetate plasma at 0.5Pa is shown in figure 1a. For this spectrum, the ion energy distribution of the protonated precursor (89 m/z) was first obtained, and the mass spectrometer then tuned to the maximum intensity in the ion energy distribution at 19eV. The dominant peak in the positive ions was the protonated precursor ion at 89 m/z, with smaller

hydrocarbon ions observed at 29, 43 and 61 m/z, with an additional peak at 19 m/z corresponding to  $\text{H}_3\text{O}^+$  which is ubiquitous and crucial for protonation in hydrocarbon plasmas.<sup>18</sup> Ions larger than the precursor molecule were also observed, with the second most intense peak assigned to the protonated dimer  $(2\text{M}+\text{H})^+$  at 177 m/z. Proposed structures for these peaks are shown in Scheme 1.



**Scheme 1.** Proposed ionic structures following protonation of ethyl acetate and subsequent collisions.

The ion energy distribution of each major peak observed in the mass spectrum was then obtained. The results in Figure 1b show that the ion energy distributions for each species overlap, with a peak centred on 19eV with a slight tail at lower ion energies. This indicates that all species are formed due to electron impacts or ion-molecule collisions in the bulk of the plasma, and they fall through the same potential difference across the sheath on approach to the surface, thus confirming the sheath is collision-less. The results for 50W plasma at the same pressure are presented in the supplementary information (Figs S1 and S2) and show similar results.

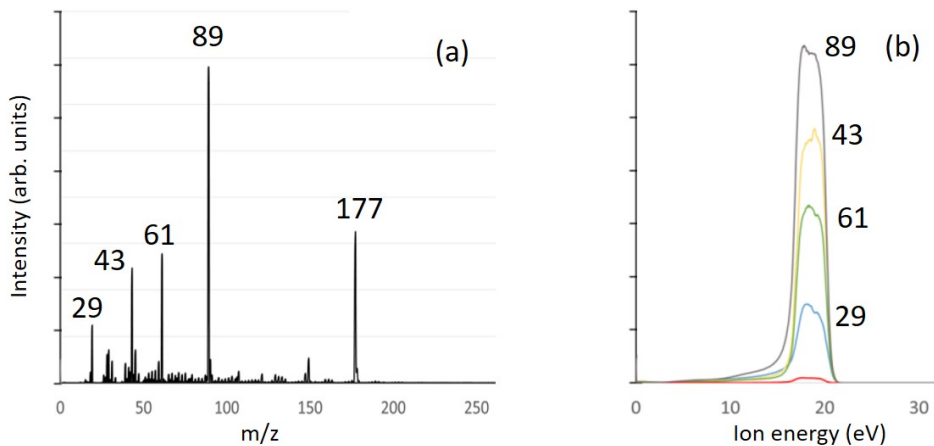


**Figure 1** (a) Positive ion plasma phase mass spectrum of ethyl acetate plasma at 10W and 0.5Pa. (b) The ion energy distributions for 29 m/z, 43 m/z, 61 m/z and 89 m/z species.

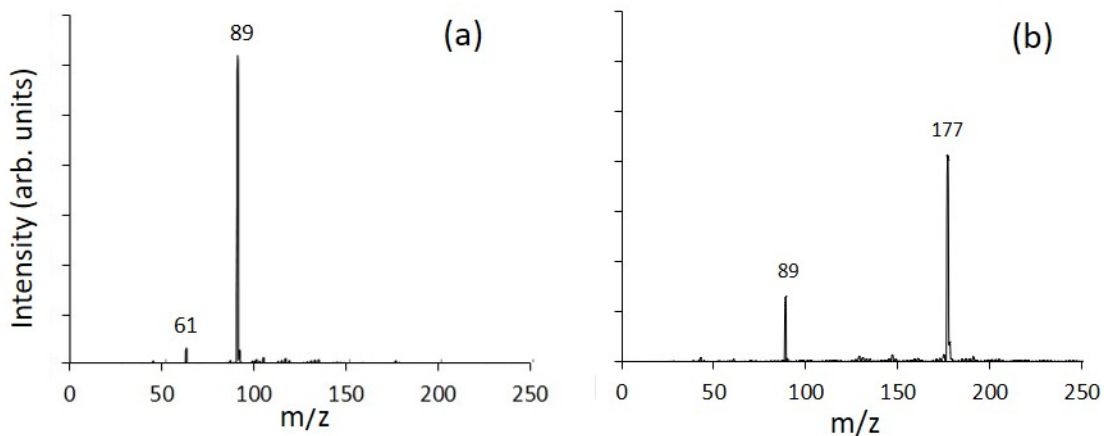


**Figure 2.** (a) Mass spectrum of 10W ethyl acetate plasma at 2Pa, with the spectrometer tuned to 11eV, corresponding to the peak in the ion energy distribution for 89 m/z. (b) mass spectrum of the same plasma with the spectrometer tuned to 17eV.

However, when the pressure is increased and the plasma enters the collisional regime, ion-molecule collisions occur in the sheath, and the ion energy is attenuated due to these collisions.

As the sheath voltage is typically  $\sim 20\text{V}$ , these collisions can be of significant energy, enough to cause bond scission and fragmentation.

Using the same technique as described above, the mass spectrum of 10W plasma at 2Pa was measured; the ion energy distribution of the protonated precursor was first measured, and the spectrometer was then tuned to the ion energy which corresponded to maximum intensity, 11eV, and finally the mass spectrum was obtained. The results in figure 2a show that the dominant peak was the protonated precursor (89 m/z) with minor peaks observed at 61 and 43 m/z. The peaks previously observed for low pressure at 29 and 177 m/z were not present. The process was then repeated for the dimer ( $[2\text{M}+\text{H}]^+$  at 177 m/z) and at the peak intensity of 17eV another mass spectrum was measured. The results in Fig 2b show a dominant peak at 177 m/z, with a much smaller peak at 89 m/z. The contrast between the spectra shows that species arriving at the surface have quite different energies, and thus are probably created in different regions of the plasma. The mass spectrometer was then tuned to each of the major peak masses observed at low pressure, and the ion energy distributions measured.

Figure 3 shows that the ion energy distribution is highly dependent on the mass of the ionic species, in contrast to the case at low pressure where the distributions overlapped. The maximum ion energy observed was at  $\sim 18\text{eV}$ , with the 29, 43, 89 and 177 m/z species all showing intensity up to this maximum energy. For these species, even though the maximum energy was common, the distributions were not the same. The protonated dimer peak (177 m/z) shows a single peak centred on 18eV, while the 89 and 61 m/z peaks exhibit maxima at 12eV and 6eV respectively. The energy distributions for 43 and 29 m/z exhibit maximum intensity at 6eV, but with local maxima at 18eV. Further increases in pressure up to 8Pa resulted in similar distributions but with a general shift to lower ion energies as shown in Fig S3.

Thus, the ion chemistry of the sheath may be quite different to that of the bulk plasma. If the energy distributions of the different ionic species are different too, then the sticking probability and ability of the impacting ions to cause sputtering and molecular rearrangements will be altered, and consequently the chemistry of the thin film will be altered.

The ion energy distributions shown in Fig 3 indicate the chemistry of the sheath region consists of several zones. Starting at the sheath – bulk plasma interface, ions entering the sheath are mainly intact precursor and dimer ions produced in the bulk of the plasma and have gained a small amount of energy as they passed through the pre-sheath (approximately 1.5 eV).<sup>19</sup> Upon entering the sheath, these ions are accelerated toward the surface by the sheath voltage and may collide with neutral species. The mean free path,  $\lambda$ , can be calculated using Eq2.<sup>19</sup>

$$\lambda = \frac{kT}{\sqrt{2}\pi d^2 p} \quad (\text{eq 2})$$

where k is Boltzmann's constant, T is the absolute temperature, d is the effective particle cross-section diameter and p is the pressure, and the probability P of an ion colliding with a neutral particle is given by Eq 3,

$$P = 1 - \exp\left(\frac{-x}{\lambda}\right) \quad (\text{eq 3})$$

where x is the distance travelled. For ethyl acetate ions at 2Pa,  $\lambda$  is approximately 1700  $\mu\text{m}$ ,<sup>20</sup> compared to the sheath thickness which is of the order of 3000  $\mu\text{m}$ .<sup>13</sup>

Therefore some ions may encounter multiple ion-molecule collisions within the sheath, while others may traverse the sheath without colliding. At low energy (a short distance into the sheath), these collisions will be elastic and result in ions arriving at the surface with attenuated



energies. However once they achieve sufficient kinetic energy, bond scission of intact ions may occur resulting in formation of smaller fragment ions. Carbon – carbon bond strengths are typically of the order of 4eV,<sup>21</sup> so ions which have gained a further 2.5eV after entering the sheath are energetic enough to cause fragmentation collisions. Assuming a sheath thickness of 3000 $\mu$ m, for a mean free path of 1700 $\mu$ m, the average collision energy is 11.9eV,

The peak at 12eV for species 89, 43 and 29 m/z represents ions created after collisions involving a 6 eV ion. These may result from fragmentation of protonated dimers (177 m/z), or protonated precursors, as shown in Scheme 2. While this is well in excess of the 4eV threshold for bond scission, the collision angle must also be taken into account using equation 4.<sup>19</sup> Assuming the neutral is of similar size to the ion and has negligible energy compared to the ion

$$E_{transfer} = E_{ion} \cos^2 \phi \quad (\text{eq4})$$

where  $E_{transfer}$  is the energy transferred during the collision,  $E_{ion}$  is the energy of the ion and  $\phi$  is the collision angle. Therefore at this energy, only collisions with angles less than  $\sim 45^\circ$  can result in bond scission. These ion fragments may then gain further kinetic energy within the sheath and secondary collisions can cause further fragmentation. Thus, the average mass of the ions decreases as the surface is approached.

The 43m/z species shows intensity from 21eV to 0eV, with a minor peak at 18eV and a major peak at 6eV. This suggests that the 43 m/z species is created in the plasma bulk due to electron impacts, but also can be the result of ion-molecule collisions within the sheath. Thus there are multiple pathways to create these ions in the plasma, resulting in a wide distribution of ion energies. This is in contrast to the protonated dimer (177 m/z) which is created in the bulk of the plasma and then fragmented within the sheath. The relatively narrow range of ion energy

distributions for this peak shows that the dimer is relatively fragile, and is not able to remain intact after collisions greater than  $\sim 8\text{eV}$ .

The spacing of these peaks is also of interest, as they occur at intervals of  $\sim 6\text{eV}$ . The ion energy distributions shown in Fig S3 and for 2Pa 50W plasma in Fig S4 also exhibit peaks separated by  $\sim 6\text{eV}$ . Due to the higher maximum ion energy in Fig S4 an extra peak is observed at 3eV.

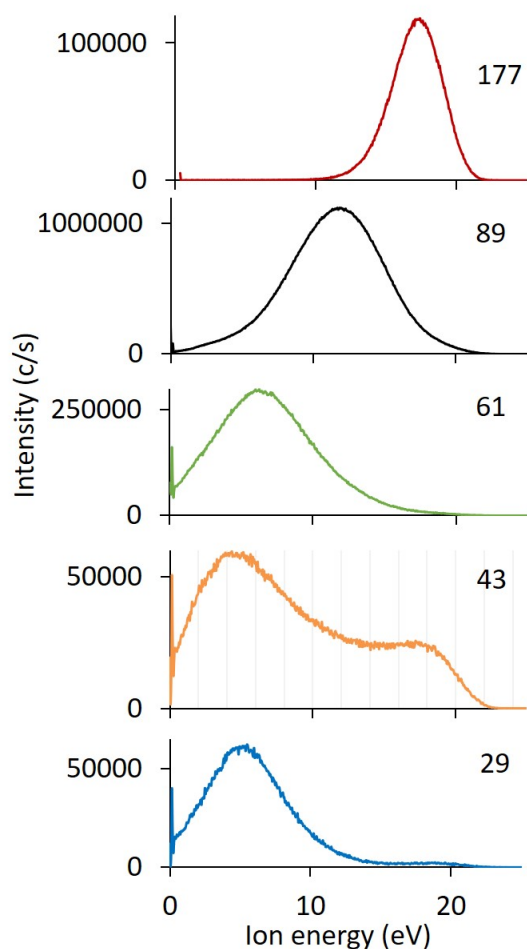
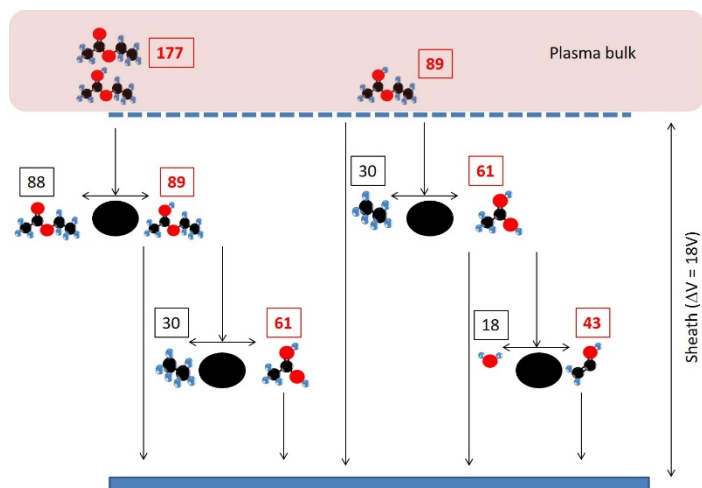


**Figure 3.** Ion energy distributions for each of the major peaks found in 2Pa 10W ethyl acetate plasma



**Scheme 2.** Examples of high energy ion – molecule collisions within the sheath which cause fragmentation and attenuation of ion energies at the surface. Ion masses are shown in red, neutral masses in black.

In summary, the chemistry of the species close to deposition surfaces in plasma changes drastically when the pressure is increased such that the sheath region becomes collisional. Below this pressure, the chemistry is determined by processes in the bulk and the ion energy is determined by the sheath potential, and is the same for all ionic species. At higher pressure, high energy collisions close to surface not only affect the chemistry of the ions, but their energy too, which has a profound effect on the chemistry of the thin film deposited, an effect which has received little attention to date. Therefore, this work identifies a new set of parameters which must be considered when optimising plasma deposition processes; it is critically important to measure the ion energy distributions of all major ionic species as this determines the deposition kinetics for each species, and surface processes such as deposition, elastic collisions or etching. Ignoring these parameters and only measuring single ion energy and mass distributions for the plasma (e.g. Figure 2a) may lead to false correlations between plasma parameters and final film quality. Ongoing investigations into these physical and chemical phenomena close to surfaces

will enable additional control of plasma processes towards improved rational control of incorporation of specific desired chemical structures in coatings. Mass spectrometry analysis of plasma phases and elucidating the role of pressure across the alpha-gamma transition, and of applied rf power, are essential aspects of work towards understanding mechanisms of plasma polymerization and guided optimization. As this study shows, the mechanistic aspects of the variable roles of various ions in plasma polymerization can be quite complex. A common method of attenuating ion energies and fragmentation in the plasma phase is to use pulsed plasma to activate the surface during the plasma on-phase via high-energy ions, which then allows radical species to deposit during the off-phase with decreased fragmentation. While this approach has been useful in improving structural retention of the precursor, the deposition rate is reduced and the lower energy density can lead to unstable films. Additionally, particularly for saturated hydrocarbons, it has been shown that protonated precursor ions with moderate ion energies are effective at retaining structural motifs<sup>22</sup>. During the on-phase, and extending into the off-phase of pulsed plasmas, the ion energies can be quite high and thus this work will be relevant to both continuous and pulsed plasma regimes.

### **Supporting Information**

Experimental methodology and equipment description. Mass spectra and ion energy distributions of 0.5Pa ethyl acetate plasma. Ion energy distributions of 10W ethyl acetate plasmas at different pressures. Ion energy distributions of 2Pa ethyl acetate plasmas at different RF powers.

### **Acknowledgements**

The authors wish to acknowledge financial support from the Australian Research Council under ARC Discovery Project DP160105001.

## References

1. Whittle, J. D.; Short, R. D.; Steele, D. A.; Bradley, J. W.; Bryant, P. M.; Jan, F.; Biederman, H.; Serov, A. A.; Choukurov, A.; Hook, A. L.; et al. Variability in plasma polymerization processes – An international round-robin study. *Plasma Processes Polym.* **2013**, *10*, 767–778.
2. Aisenberg, S.; Chabot, R. Ion-Beam Deposition of Thin Films of Diamondlike Carbon. *J. Appl. Phys.* **1971**, *42*, 2953-2958
3. Dobbelaere, T.; Roy, A.K.; Vereecken, P.; Detavernier, C. Atomic Layer Deposition of Aluminum Phosphate Based on the Plasma Polymerization of Trimethyl Phosphate. *Chem. Mater.* **2014**, *26*, 6863-6871
4. Khelifa, F.; Ershov, S.; Habibi, Y.; Snyders, R.; Dubois, P. Free-radical-induced grafting from plasma polymer surfaces, *Chem. Rev.* **2016**, *116*, 3975-4005
5. Bazaka, K.; Jacob, M.W.; Chrzanowski, W.; Ostrikov, K. Anti-bacterial surfaces: natural agents, mechanisms of action, and plasma surface modification. *RSC Adv.* **2015**, *5*, 48739-48759
6. Alf, M.E.; Asatekin, A.; Barr, M.C.; Baxamusa, S.H.; Chelawat, H.; Ozaydin-Ince, G.; Petruczok, C.D.; Sreenivasan, R.; Tenhaeff, W.E.; Trujillo, N.J.; Vaddiraju, S.; Xu, J.; Gleason, K.K. Chemical vapor deposition of conformal, functional, and responsive polymer films, *Adv. Mater.* **2010**, *22*, 1993-2027

7. Friedrich, J. Mechanisms of Plasma Polymerization – Reviewed from a Chemical Point of View. *Plasma Processes Polym.*, **2011**, *8*, 783–802
8. Padron-Wells, G.; Jarvis, B.C.; Jindal, A.K.; Goeckner, M.J. Understanding the Synthesis of DEGVE Pulsed Plasmas for application to ultra thin biocompatible interfaces. *Colloids Surf. B*, **2009**, *68*, 163–170.
9. Perrin J. Plasma and surface reactions during a-Si:H film growth. *J Non Cryst Solids*. **1991** *137–8*, 639–44.
10. Michelmore, A.; Steele, D. A.; Whittle, J. D.; Bradley, J. W.; Short, R. D. Nanoscale Deposition of Chemically Functionalised Films via Plasma Polymerisation. *RSC Adv*. **2013**, *3*, 13540–13557
11. Ryssy, J.; Prioste-Amaral, E.; Assuncao, D.F.N.; Rogers, N.; Kirby, G.T.S.; Smith, L.E.; Michelmore, A. Chemical and physical processes in the retention of functional groups in plasma polymers studied by plasma phase mass spectroscopy. *Phys. Chem. Chem. Phys.* **2016**, *18*, 4496-4504
12. Liu, X.; Feng, Q.; Bachhuka, A.; Vasilev, K. Surface chemical functionalities affect the behavior of human adipose-derived stem cells in vitro. *App. Surf. Sci.* **2013**, *270*, 473-479
13. Lieberman, M.A.; Lichtenberg, A. J. Principles of plasma discharges and materials processing, John Wiley & Sons, New Jersey, 2005.

14. Saboohi, S.; Jasieniak, M.; Coad, B.R.; Griesser, H.J.; Short, R.D.; Michelmore, A. Comparison of plasma polymerization under collisional and collision-less pressure regimes. *J. Phys. Chem. B.* **2015**, *119*, 15359-15369
15. Saboohi, S.; Coad, B.R.; Griesser, H.J.; Michelmore, A.; Short, R.D. Synthesis of highly functionalised plasma polymer films from protonated precursor ions via the plasma  $\alpha$ - $\gamma$  transition. *Phys. Chem. Chem. Phys.* **2017**, *19*, 5637-5646
16. Buddhadasa, M.; Lerouge, S.; Girard-Lauriault, P-L. Plasma polymer films to regulate fibrinogen adsorption: Effect of pressure and competition with human serum albumin. *Plasma Process Polym.* **2018**, *15*, e1800040.
17. Jacobs, D.C. Reactive Collisions of Hyperthermal Energy Molecular Ions with Solid Surfaces. *Annu. Rev. Phys. Chem.* **2002**, *53*, 379-407.
18. Saboohi, S.; Griesser, H.J.; Coad, B.R.; Short, R.D.; Michelmore, A. Promiscuous hydrogen in polymerising plasmas. *Phys. Chem. Chem. Phys.* **2018**, *20*, 7033-7042
19. Chapman, B. Glow Discharge Processes, John Wiley and Sons, Chichester, 1980.
20. de Souza, G.L.C.; da Silva, L.A.; de Sousa, W.J.C.; Sugohara, R.T.; Iga, I.; dos Santos, A.S.; Machado, L.E.; Homem, M.G.P.; Brescansin, L.M.; Lucchese, R.R.; Lee, M.-T. Electron collisions with small esters: A joint experimental-theoretical investigation, *Phys. Rev. A.* **2016**, *93*, 032711
21. Blanksby, S.J.; Ellison, G.B. Bond Dissociation Energies of Organic Molecules. *Acc. Chem. Res.* **2003**, *36*, 255-263

22. Saboohi, S.; Coad, B.R.; Michelmore, A.; Short, R.D.; Griesser, H.J..  
Hyperthermal Intact Molecular Ions Play Key Role in Retention of ATRP Surface  
Initiation Capability of Plasma Polymer Films from Ethyl  $\alpha$ -Bromoisobutyrate. *ACS Appl.  
Mater. Interfaces*. **2016**, 8, 16493-16502